

ISUAAAT15-079

FLUCTUATING INFLOW CONDITIONS FOR TIME-DOMAIN BOUNDARY ELEMENT METHOD FOR AIRFOIL-TURBULENCE INTERACTION NOISE

Sparsh Sharma

Technical Acoustics, Brandenburg Technical University
Cottbus-Senftenberg
Cottbus, Germany

Ennes Sarradj

Technical Acoustics, Technical University - Berlin
Berlin, Germany

ABSTRACT

Acoustic radiation from an airfoil subjected to a real flow is one such effect induced by turbulence and demands high-performance computing for its prediction numerically. The methods which are available now range back from analytical ones, which are fast but not precise enough to capture nonlinear effects, to the numerical one, which heavily depends on the computing resources. This study focuses on the development, validation, and demonstration of a transient, two-dimensional stochastic method for the prediction of leading edge noise. A new approach to model the noise from turbulent flows is presented to bridge the low fidelity and high-fidelity methods. The method relies on the classical view of turbulence as a superposition of random vortices convected with the mean flow. The fluctuating velocity is formulated using the scalar potential given by a convolution product which furnishes a solenoidal velocity field. The system is then optimised stochastically to create a realistic turbulence field based on a target energy spectra using an evolutionary optimisation algorithm. The pressure signals are then used to calculate the sound radiation using Ffowcs-Williams and Hawking's analogy. The approach has been validated against analytical solutions of the linearized wave equations and experimental data available.

INTRODUCTION

The noise due to the interaction of turbulent flow with the leading edge of an airfoil is a primary source of aerodynamic noise. The problem is illustrated in Fig. 1. Turbulence is, by its very nature, stochastic and therefore has a broad frequency spectrum which makes it more difficult to calculate the effect induced by it. Acoustic radiation from an airfoil subjected to a real flow is one such effect induced by turbulence and demands high-performance computing for its prediction numerically. The methods which are available now range back from analytical ones, which are fast but not precise enough to capture nonlinear effects, to the numerical one, which heavily depends on the computing resources [1].

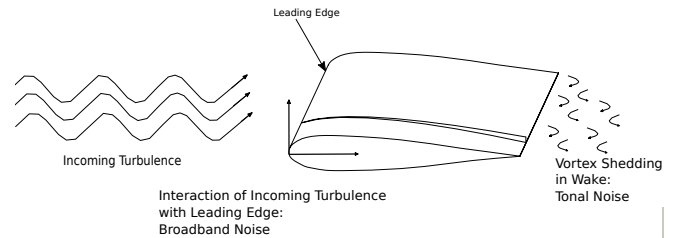


Figure 1: Incidence turbulence interacting with the leading edge of an airfoil

The early studies by [2], [3], and [4] show the use of frequency domain analysis which have accounted for the effects of thickness, camber, and angle of attack, but were mainly used for relatively low frequencies. As the frequency increases, the spatial and temporal resolution requirements make these numerical methods more difficult to apply [5]. Another prevalent method in use is the time domain analysis [6-8] which uses a set of discrete vortices to realise the turbulent inflow. This method has an advantage over the frequency domain, primarily the ability to realise the turbulent inflow with the desired statistical properties. On another hand, it is way more challenging to model the inflow conditions using a set of discrete vortices, since the parameters which control the size and the strength of these vortices are unknown.

Among the different available methods to synthesise synthetic turbulent flow signal, a method proposed by [9], of superimposing a white noise signal over the mean flow. [10], [11], and [12] used a similar method to realise a two-dimensional synthetic turbulent inflow using the point vortices. [13] studied the behaviour of a finite number of point vortices and examined the possibility of replacing a turbulent flow with a collection of point vortices. However, there is a problem with approximating the vorticity with point vortices (delta functions), i.e. infinite spikes, which is an associated singularity in the streamfunction and velocity

fields. This singularity appears when the distance to the point vortex becomes very small.

The main objectives of this paper are to overcome this difficulty by replacing the point-vortices with the shape function vortices with the details of their implementation, and to optimise these shape function vortices in order to obtain a realistic 2D von Kármán energy spectra. Section *Numerical method* presents the kinematics of the vortex particles and the governing equations involved in the Lagrangian frame of reference. The singularity associated with the point vortices as well as its elimination is discussed in *Point vortex singularity and Gaussian wave shape function* followed by the synthesis of the turbulent inflow in *Synthesis of 2D turbulence*.

NUMERICAL METHOD

Vortex particle kinematics

Consider two-dimensional flows, where the incompressibility constraint $\nabla \cdot u = 0$ is satisfied by taking $u_1 = -\partial\psi/\partial y$, $u_2 = \partial\psi/\partial x$. The stream function $\psi(x, t)$ (which is a conserved quantity [14]) plays the role of the Hamiltonian for the coordinates (x, y) of the vortex particle whose dynamics is given by

$$\frac{dx_i}{dt} = \frac{d\psi}{dy_i}, \quad \frac{dy_i}{dt} = -\frac{d\psi}{dx_i}, \quad (1)$$

and can be written as

$$\psi(r_1, \dots, r_N) = -\sum_{i=1}^N \sum_{j=i+1}^N \Gamma_i \Gamma_j G(r_i, r_j) - \frac{1}{2} \sum_{i=1}^N \Gamma_i^2 g(r_i, r_i), \quad (2)$$

where Γ represents the circulation. The first term on the right hand side is the Green's function of the first kind for the domain, defined by

$$\mathcal{L}G(r, r') = \delta(r, r'). \quad (3)$$

\mathcal{L} , the linear elliptic operator is taken to be the Laplacian ($\mathcal{L} \equiv \Delta$, for most of the formulations), and the result is the point vortex dynamical system of the 2D Euler equations. The second term, $g(r, r')$, is the residual Green's function defined by

$$g(r, r') = G(r, r') - G_0(r, r'), \quad (4)$$

where G_0 corresponds to the free space Green's function. Numerical solution of the system Eq. (1) has understandably focused on the 2D Euler system, for which

$$\mathcal{L} \equiv \Delta, \quad G_0(r, r') = \frac{1}{2\pi} \log(|r - r'|). \quad (5)$$

The Green's function formulation for \mathcal{L} , the linear elliptic operator, Eq.(5) is an important result which is used in next section.

Governing equation

Two-dimensional ideal flows are ruled by Euler equation that, in terms of the vorticity $\omega \hat{z} = \nabla \times u$ (which is perpendicular to the plane of the flow), expressing the conservation of vorticity along fluid-element paths. The velocity and the vorticity field is described with the aid of a single scalar streamfunction ψ . Writing the velocity in terms of the streamfunction, $u = \nabla^\perp \psi = (u_1 = \partial\psi/\partial y, u_2 = -\partial\psi/\partial x)^T$, the vorticity is given by

$$\omega = -\Delta\psi, \quad (6)$$

where Δ is the Laplacian operator. The single streamfunction ψ unifies the streamfunctions for each constituent of the flow field, ψ_ω the vorticity of the flow field and the solid body rotation, ψ_γ the vortex sheet distribution on the boundary (body), and ψ_∞ corresponding to the velocity field at infinity. Applying the Poincaré identity to each component of the streamfunction ψ yields [15]

$$\begin{aligned} \psi(r, t) = & \underbrace{\int \frac{\omega(r', t) G(r, r') dr'}{\psi_\omega}}_{\psi_\omega} \\ & + \underbrace{\int \left[\left(\frac{\partial(\psi_o - \psi_i)}{\partial n}(r') G(r, r') \right) - \left((\psi_o - \psi_i)(r') \frac{\partial G}{\partial n}(r, r') \right) \right] dr'}_{\psi_\gamma} \\ & + \psi_\infty, \end{aligned} \quad (7)$$

where $G(r, r') = \frac{1}{(2\pi)\log(|r - r'|)}$ is the Green's function of the Laplacian operator Δ , $r = (x, y)$ is a point in the flow field, and r' is the location of the vortex. The above equation (Eq. (7)) can be expressed in terms of singularity distributions on the boundary of the domain for which the source distribution and the vortex sheet are defined as $\sigma = \psi_o - \psi_i$ and $\gamma = \frac{\partial\psi_o}{\partial n} - \frac{\partial\psi_i}{\partial n}$, respectively. The subscript o and i represent the area outside the body and the area inside the body, respectively in the domain. Therefore, the velocity can be expressed in terms of ω as [9, 16],

$$u_\omega(r, t) = \nabla^\perp \int G(r, r') \omega(r', t) dr', \quad (8)$$

$$u_\gamma(r, t) = \nabla^\perp \int \left[\gamma(r') G(r, r') - \sigma(r') \frac{\partial G}{\partial n}(r, r') \right] dr', \quad (9)$$

The discretized vorticity field is expressed as the sum of the vorticities of the N vortex particles, in which the initial circulation Γ is concentrated, in the following way:

$$\omega(r, t) = \sum_{n=1}^N \Gamma_n \delta(r - r_n(t)), \quad (10)$$

where $n \in \{1, \dots, N\}$ is an index to denote each individual vortex. Vorticity is created continuously at the fluid-solid interface as a consequence of continuously satisfying the surface velocity boundary conditions. These conditions are enforced at the boundary elements (panels), which are the discretized surface into N panels of a certain length and enforces the no-slip and no-penetration boundary conditions at the centre point of each panel. The domain is discretized

into computational nodes, interpreted as either of sources, doublets, vortex particles or the combination of two or all [17]. The surface (sheet) circulation computed by the BEM is then released into the flow at each time step as new circulation-carrying particles (vortices).

Point vortex singularity and Gaussian wave shape function

The resulting velocity field (Eq. (8)) induced by the point-vortices raises no problem when used as the singularity distribution on the domain boundaries or/and as the circulation carrier at each time-step, however, [13, 18] showed, in their work on point vortices to realise a white noise signal, that there exists a problem when approximating the vorticity with delta functions (point vortices), i.e. infinite spikes, which is an associated singularity in the streamfunction and velocity field. This singularity appears when the distance to the point vortex becomes very small. This is quite problematic in the evaluation of the sums. It is, therefore, becomes necessary to eliminate the "spiky" representation of the vorticity. In this paper, a method based on the shape function vortices is adopted to handle these infinite spikes which was first proposed by [19] which was later developed by [20] who showed that this shape function signal satisfies the convecting equations based on the mean flow which means that scalar potential is convected by the mean flow. The shape function vortices have a finite core which eliminates the associated singularity. The shape function can either be a Gaussian wave or a Mexican hat wavelet or a Morlet wavelet, or a combination of two or all. To build these representations, it is thus assumed that each of the finite-core vortices is associated with a localised shape function, $\psi = f(r)$ that is radially symmetric about the centre of the vortex, that decays as we move away from the centre, and whose integral over the entire plane is unity. For the current study, the shape function considered for the vortices is the Gaussian wave which is given by

$$\psi(\mathbf{r}, t) = \gamma^{-\frac{1}{2}} e^{-(3\mathbf{r})^2}, \quad (11)$$

where the right-hand side is a transcendental function, called the shape function (a spatiotemporal polynomial), with γ as the directional strength of the vortex, controls the size of the vortex (radius of the vortex core, $R = 1/\sqrt{\gamma}$), \mathbf{r} is the position of the vortex in the computational domain.

Since the method is based on an unbounded domain contrary to the synthetic eddy modelling which requires the definition of a precise volume (area for 2D) containing all the turbulent structures, a finite domain of interest is defined and named as *vortices window*. The vortices are randomly distributed in this two-dimensional finite space, as shown in Fig. 2, and are convected along with the mean flow. A general form of the scalar potential, ψ_{turb} , for such a space can be written as:

$$\psi_{turb}(r, t) = \sqrt{\frac{A_{inflow}}{N}} \sum_{n=1}^N \varepsilon_n \psi_n \left(\frac{|r-r'|}{L_b}, \frac{t-t'}{\tau_b} \right), \quad (12)$$

where A_{inflow} is the area of the vortices window, N is the total number of vortices. $\sqrt{(A_{inflow}/N)}$ indicates the average distance between two adjacent vortices inside the vortices window. ε_n is a random sign switch taking the value of -1 or 1, ψ_n represents a dimensionless shape function for each individual vortex. r' is the spatial and t' is the temporal location of the vortex. L_b and τ_b denotes the turbulent length and time scales, respectively.

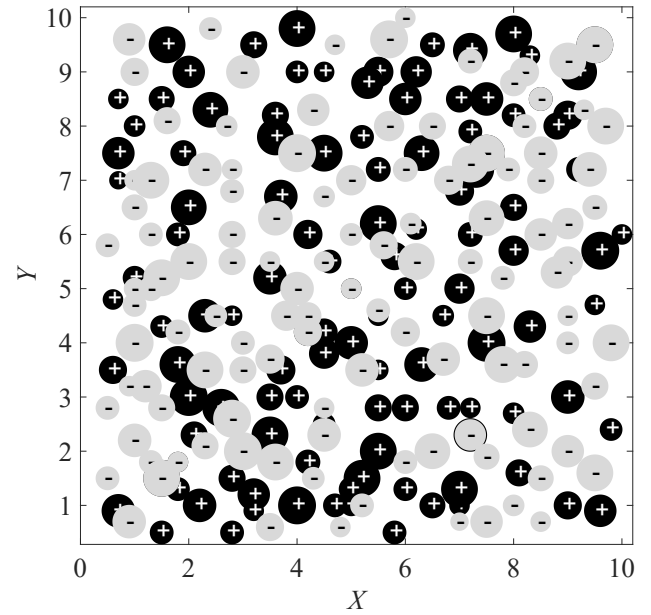


Figure 2: Distribution of the vortices are indicated by discs with area proportional to the vortex intensity, gray symbols indicate the negative (clockwise flow), and the black symbols indicate positive (counter-clockwise flow) circulation, respectively

SYNTHESIS OF 2D TURBULENCE

Controlling parameters

The next objective of the present study is to realise a realistic turbulent velocity field from the shape function vortices which then can be used to calculate the leading-edge noise. As turbulence is, by its very nature, stochastic and therefore modelling it using a set of discrete vortices require few constraints to regulate them to employ the stochasticity. A total of 6 constraint parameters, listed in table 1, are introduced to control and optimise the overall distribution of random vortices to replicate a target energy spectra, von Kármán energy spectra, for a homogeneous isotropic two-dimensional turbulence. Using Eqs. (11) and (12), a Gaussian profile scalar potential can be written as

$$\psi_{turb}(r, t) = \sqrt{\frac{A_{inflow}}{N}} \sum_{n=1}^N \varepsilon_n [(\gamma_n \rho_n^{-1/2} e^{-(3\rho_n r_n)^2})]. \quad (13)$$

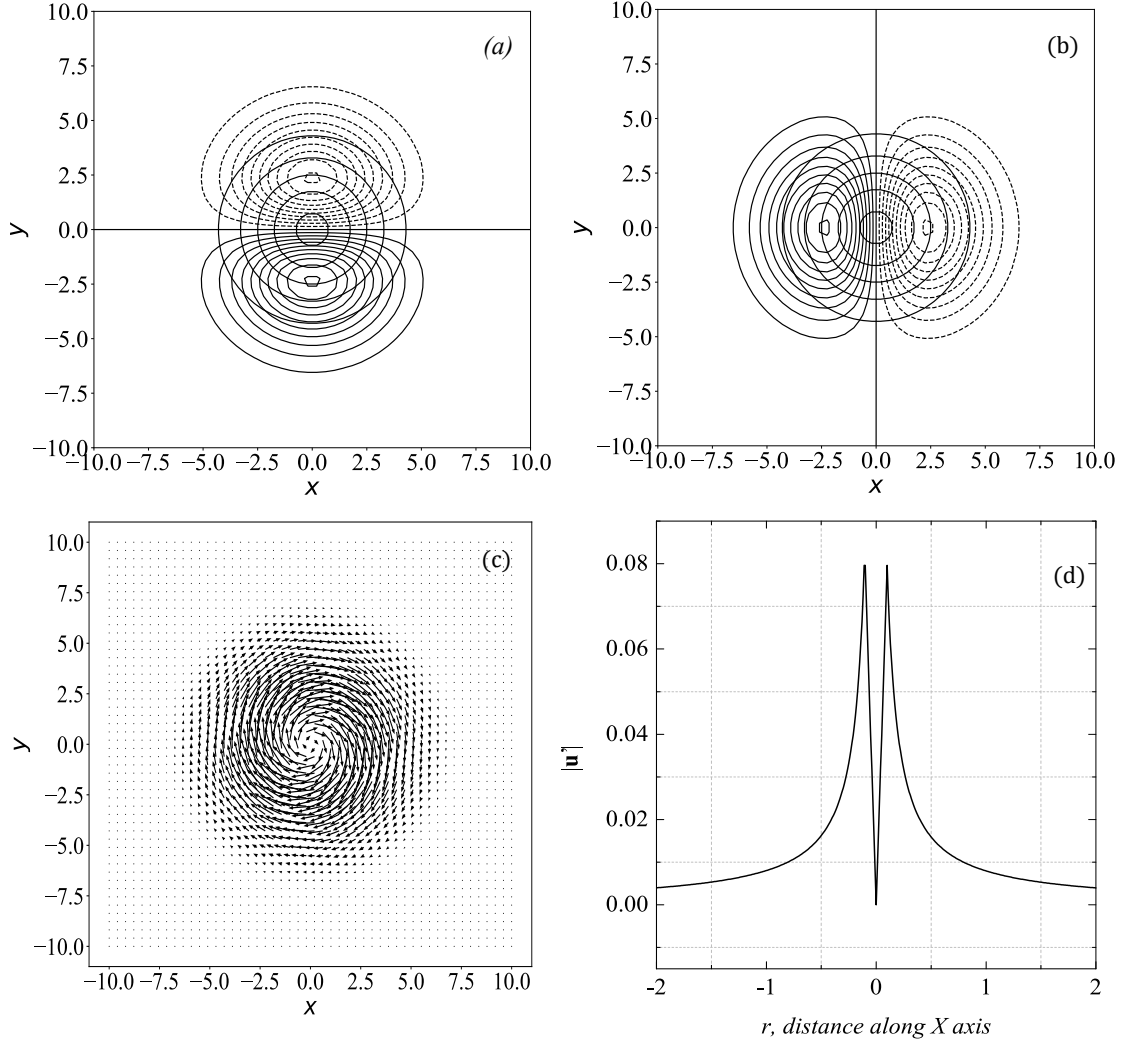


Figure 3: (a) u_1 contours and streamlines, (b) u_2 contours and streamlines, (c) velocity vector quiver plot, (d) velocity profile of the Gaussian wavelet

Table. 1 Parameters controlling the turbulence statistics

| Parameters | Definition | Values |
|----------------|--|------------|
| N | Number of the vortices in the vortex window | 100(fixed) |
| A_{inflow} | Area of the vortex window (2(chordlength)) (fixed) | |
| R_{max} | Upper limits for the vortex size (radius) | 0.5 |
| R_{min} | Lower limits for the vortex size (radius) | 0.1 |
| γ_{max} | Upper limits in eddy strength in the x-direction | 0.01 |
| γ_{min} | Lower limits in eddy strength in the x-direction | -0.01 |

The resulting fluctuating velocity field for a new vortex profile is obtained by introducing Eq. (13) into $u = \nabla^\perp \psi$ at (x_0, y_0)

$$u_1(\mathbf{r}, t) = \frac{\partial \psi_{turb}(\mathbf{r}, t)}{\partial y} = -18 \sqrt{\frac{A_{inflow}}{N}} \sum_{n=1}^N \varepsilon_n [(\gamma_n \rho_n^{3/2} e^{-9\rho_n^2 r_n^2})(y - y_0)], \quad (14)$$

$$u_2(\mathbf{r}, t) = -\frac{\partial \psi_{turb}(\mathbf{r}, t)}{\partial x} = 18 \sqrt{\frac{A_{inflow}}{N}} \sum_{n=1}^N \varepsilon_n [(\gamma_n \rho_n^{3/2} e^{-9\rho_n^2 r_n^2})(x - x_0)]. \quad (15)$$

The velocity contours with streamlines and the normalised velocity magnitude of a two-dimensional Gaussian vortex, according to Eqs. (14) and (15) with $N = 1$, are shown in Fig. 3.

Homogeneous and Isotropic Two-Dimensional Turbulence

The constrained parameters (listed in table 1) define the scalar potential (Eq. 13) which is used to calculate the numerical spectra. The study of homogeneous and isotropic turbulence is supported by the use of correlation functions. For a two-dimensional incompressible flow, the two-point two-time correlation tensor of the turbulent velocity u is defined as $\mathcal{R}_{ij}(\mathbf{r}, \tau) = \langle u_i(\mathbf{r}_1, t_1) u_j(\mathbf{r}_2, t_2) \rangle$, where $\langle \cdot \rangle$ denotes the ensemble average, $\mathbf{r} = |\mathbf{r}_1 - \mathbf{r}_2|$ and $\tau = |t_1 - t_2|$. The velocity field is defined in terms of a scalar field $\psi_{turb}(\mathbf{r}, t)$, which is modelled as a homogenous, isotropic, and stationary Gaussian stochastic process. The correlation of the streamfunction can be written as

$$\mathcal{C}_{ij}(\mathbf{r}, \tau) = \langle \psi_{turb,i}(\mathbf{r}_1, t_1) \psi_{turb,j}(\mathbf{r}_2, t_2) \rangle. \quad (16)$$

[21] showed that C is related to the radial correlation function \mathcal{R} using $u = \nabla^\perp \psi$ and using the properties of the Bessel functions as

$$\mathcal{R}(r) = \frac{1}{2} \mathcal{R}_{ij}(r, 0) = \frac{1}{4\pi} \int_0^\infty k^3 \hat{\mathcal{C}}(k) J_0(kr) dk, \quad (17)$$

where $\hat{\mathcal{C}}$ is the Fourier transform of the correlation function C , $r = |\mathbf{r}|$ and $k = |\mathbf{k}|$. J_0 is the Bessel function of the zeroth order. Correspondingly, $\hat{\mathcal{C}}$ to the energy spectrum $E(k)$ of the turbulence is related as [21]

$$E(k) = \frac{1}{4\pi} k^3 \hat{\mathcal{C}}(k). \quad (18)$$

Kraichnan [9] proposed the fluctuating velocity field, u can be expressed as

$$u(\mathbf{r}, t) = \nabla^\perp \underbrace{\int \mathcal{G}(\mathbf{r}, \mathbf{r}') \mathcal{U}(\mathbf{r}', t) d\mathbf{r}'}_{\psi_{turb}}, \quad (19)$$

where \mathcal{G} is a spatial Green's function filter, $\mathcal{U} = (U_1, U_2, U_3)$ is the white noise field which is reduced to a single term, $\mathcal{U} = (0, 0, U_3)$, for a two-dimensional turbulent flow. Following [22], it is possible to express the streamfunction correlation in terms of the filter as the convolution of the temporal correlation of \mathcal{U} which leads to relate the Fourier transform \hat{G} of the filter to the energy spectrum:

$$E(k) = \frac{1}{4\pi} k^3 \hat{G}(k)^2. \quad (20)$$

The resulting numerical spectra for fluctuating velocity is obtained by introducing Eq. (13) into Eq. (20) as

$$E(k) = \frac{1}{4\pi} k^3 \frac{A_{inflow}}{N} \sum_{i=1}^N \sum_{j=1}^N \frac{\gamma_i \gamma_j}{18 \sqrt{\rho_i^3 \rho_j^3}} \exp \left[-\frac{k^2}{18(\rho_i^2 + \rho_j^2)} \right]. \quad (21)$$

Target spectra: Homogeneous and Isotropic Two-Dimensional Turbulence

The target spectra $E_{tar}(k)$ for the numerical spectra $E(k)$ is von Kármán energy spectra for two-dimensional homogenous isotropic turbulence which is given by [23],

$$E_{tar}(k) = E^{VK}(k) = \frac{110 u_{rms}^2 \Lambda}{27\pi} \frac{\left(\frac{k}{k_c}\right)^4}{\left[1 + \left(\frac{k}{k_c}\right)^2\right]^{17/6}}, \quad (22)$$

$$k_c = \frac{\Gamma\left(\frac{1}{2}\right) \Gamma\left(\frac{5}{6}\right)}{\Lambda \Gamma\left(\frac{1}{3}\right)}.$$

where Λ is the integral length scale, Γ is the gamma function.

In the present study, the vortices window is injected close to the leading edge of the airfoil. $u_{rms}/u_\infty = 0.04$ which is equivalent to 4.0% turbulence intensity and $\Lambda = 0.058$, corresponds to the length scale are set as the parameters for the target energy spectra.

STOCHASTIC OPTIMISATION: GENETIC ALGORITHM

The ability of the numerical turbulence to realise the desired statistical properties relies on the optimisation of 6 constrained parameters

$$\mathcal{P} = (N, A_{inflow}, R_{max}, R_{min}, \gamma_{max}, \gamma_{min}). \quad (23)$$

The optimisation of these parameters is carried out by defining an error function as

$$\varepsilon(\mathcal{P}) = \left| \log_{10} \frac{\langle E(k) \rangle}{E^{VK}(k)} \right| \quad (24)$$

The $E(k)$ spectra, given by Eq. (21), are optimised to $E^{VK}(k)$ for k values from 1 to 150 by minimising the error function $\varepsilon(\mathcal{P})$. The value of N is fixed at 100. An evolution-based optimisation technique, Genetic algorithm, is used to minimise the error function. The algorithm takes random values within the identified range for the constrained parameters, and the process is repeated until the best fitting spectra are obtained. For the current parameters, the algorithm converges to the optimal value after 100 iterations with an initial population of 200.

The target spectra for the turbulent inflow is shown in the Fig. 4. The numerical and experimental [24] spectra are in good agreement with the corresponding target one.

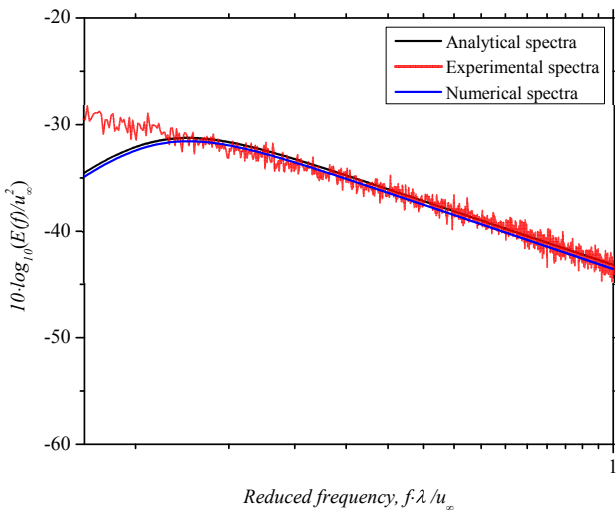


Figure 4: Energy spectra comparison with black line representing analytical spectra, red line representing experimental spectra, and blue line representing optimised numerical spectra

RESULTS AND DISCUSSION

The objectives of the present paper, to overcome the singularity associated with the point vortices and the realisation of a statistically matched spectra, are successfully met. In contrast, this also shows that it is relatively easy as well as computationally economic to model the turbulent inflow conditions for a time-domain analysis over a vast range of wavenumbers.

In this paper, a scalar potential using a Gaussian wave shape function is derived to construct a stochastic function for the calculation of energy spectra. The Gaussian profile for the vortices eliminates the problem of infinite spikes when the distance to the vortex becomes very small. The derived spectral equations for the energy has the same structure as the spectral equations of [25]. The optimisation of the constrained parameters is performed using the genetic algorithm which enhances the randomness in the system. The vortices are distributed in the model with the average separation between two adjacent vortices less than a fixed critical distance. Using the optimised constraint parameters for $Tu=4\%$ and length scale = 5.8 mm, the contour plot of the vorticity field in two-dimensions is shown in Fig. 5.

This low-cost methodology aims at providing a realistic and statistically optimised turbulent inflow conditions for the broadband noise calculation using a vortex method. It uses a Gaussian shape waveform to construct the spatial filter, however, an advanced scalar potential (vector potential for three-dimensional analysis) can be constructed using different available shape functions.

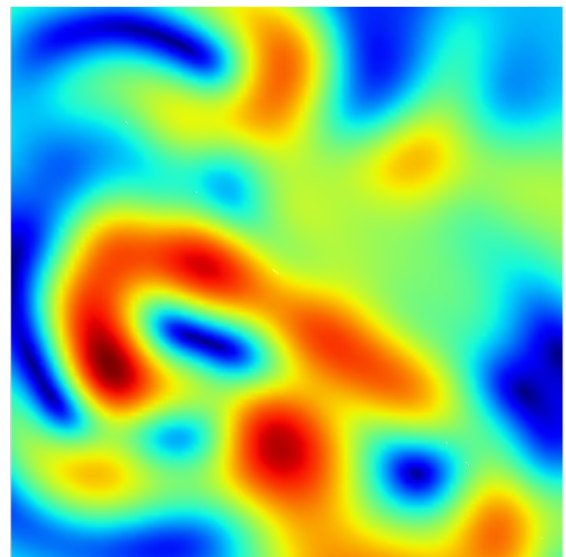


Figure 5: snapshot of vorticity at an instant

REFERENCE:

- [1] S Sharma, E Sarradj, H Schmidt, "Low-Fidelity Stochastic Approach for Airfoil-Turbulence Interaction Noise", DAGA 2018 - 44. JAHRESTAGUNG FÜR AKUSTIK, München Germany, 1184-1187
- [2] P. E. Doak, "Acoustic radiation from a turbulent fluid containing foreign bodies," Proceedings of the Royal Society A: Mathematical, Physical and Engineering Sciences 254 (1960).
- [3] I. J. Sharland, "Sources of Noise in Axial Flow Fans," Journal of Sound and Vibration 1, 302-322 (1964).
- [4] R Amiet and W. R. Sears, "The aerodynamic noise of small-perturbation subsonic flows," Journal of Fluid Mechanics 44, 227-235 (1970).
- [5] Peter D. Lysakn, Dean E. Capone, and Michael L. Jonson, "Prediction of high frequency gust response with airfoil thickness effects," Journal of Fluids and Structures 39, 258-274 (2013).
- [6] Massimo Gennaretti and Giovanni Bernardini, "Novel Boundary Integral Formulation for Blade-Vortex Interaction Aerodynamics of Helicopter Rotors," AIAA Journal 45, 1169-1176 (2007).
- [7] Donald Rockwell, "VORTEX-BODY INTERACTIONS," Annual Review of Fluid Mechanics 30, 199-229 (1998).
- [8] M. Gennaretti, L. Luceri, and L. Morino, "A unified boundary integral methodology for aerodynamics and aeroacoustics of rotors," Journal of Sound and Vibration 200, 467-489 (1997).

- [9] Robert H. Kraichnan, "Diffusion by a Random Velocity Field," *Physics of Fluids* 13, 22 (1970).
- [10] David M. F. Chapman, "Ideal vortex motion in two dimensions: Symmetries and conservation laws," *Journal of Mathematical Physics* 19, 1988 (1978).
- [11] R. Benzi, S. Succi, and M. Vergassola, "The lattice Boltzmann equation: theory and applications," *Physics Reports* 222, 145-197 (1992).
- [12] Dalila Elhmaidi, Antonello Provenzale, and Armando Babiano, "Elementary topology of two-dimensional turbulence from a Lagrangian viewpoint and single-particle dispersion," *Journal of Fluid Mechanics* 257, 533 (1993).
- [13] J. G. Esler and T. L. Ashbee, "Universal statistics of point vortex turbulence," *Journal of Fluid Mechanics* 779, 275-308 (2015).
- [14] Cencini, Massimo, Cecconi, Fabio & Vulpiani, Angelo 2010 Chaos From Simple Models to Complex Systems, arXiv: arXiv:1011.1669v3.
- [15] Georges-Henri Cottet and Petros D. Koumoutsakos, *Vortex methods : theory and practice* (Cambridge University Press, 2000) p. 313.
- [16] Alexandre J. Chorin, *Vorticity and Turbulence*, Vol. 103 (Springer New York, New York, NY, 1994).
- [17] Joseph Katz and Allen Plotkin, Cambridge University Press, February 2013 (Cambridge University Press, Cambridge, 2001) p. 351.
- [18] B N Kuvshinov and T J Schep, "Point-Vortex Approach in Two-Dimensional Turbulence 1," 42, 523 {536 (2016).
- [19] N. Jarrin, S. Benhamadouche, D. Laurence, and R. Prosser, "A synthetic-eddy-method for generating inflow conditions for large-eddy simulations," *International Journal of Heat and Fluid Flow* 27, 585-593 (2006).
- [20] Adrian Sescu and Ray Hixon, "Toward low-noise synthetic turbulent inflow conditions for aeroacoustic calculations," *International Journal for Numerical Methods in Fluids* 73, 1001-1010 (2013).
- [21] A. Careta, F. Gagues, and J. M. Sanch, "Stochastic generation of homogeneous isotropic turbulence with well-denied spectra," *Physical Review E* 48, 2279-2287(1993).
- [22] M. Dieste and G. Gabard, "Random particle methods applied to broadband fan interaction noise," *Journal of Computational Physics* 231, 8133-8151 (2012).
- [23] Christophe Bailly and Genevieve Comte-Bellot, *Turbulence*, 2015
- [24] Till Biedermann, Pasquale Czeckay, Thomas F. Geyer, Frank Kameier, and Christian O. Paschereit. "Noise Source Identification of Aerofoils Subjected to Leading Edge Serrations using Phased Array Beamforming", 2018 AIAA/CEAS Aeroacoustics Conference, AIAA AVIATION Forum, (AIAA 2018-3794)
- [25] Fernando Gea-Aguilera, James Gill, and Xin Zhang, "Synthetic turbulence methods for computational aeroacoustic simulations of leading edge noise," *Computers and Fluids* 157, 240-252 (2017).